# COMBINATION SHEAR-COMPRESSION TESTING OF FOAM MATERIALS FOR THEIR APPLICATION IN BICYCLE HELMETS OR OTHER COMPLEXLY LOADED STRUCTURES

K. VandenBosche[1], J. Ivens*[1,2], I. Verpoest[1], J. Goffin[3], G. Van der Perre[4], J. Vander Sloten[4]
1: Department of Metallurgy & Materials Engineering, Katholieke Universiteit Leuven, Belgium
2: Department of Applied Engineering, Lessius University College, Belgium
3: Experimental Neurosurgery and Neuroanatomy, Katholieke Universiteit Leuven, Belgium
4: Biomechanics and Engineering Design, Katholieke Universiteit Leuven, Belgium
* Corresponding author (jan.ivens@mtm.kuleuven.be)

## 1 Introduction

The shear properties of the foam cushioning material in a bicycle helmet can be correlated to the resulting rotational acceleration of the head during impact. This rotational acceleration is known to cause significant brain injuries, and should be minimized [1, 2]. It is therefore important to study the shear behavior of helmet foams. Bicycle helmet foam, however, never experiences purely shear or compression deformation. Impacts are generally oriented at oblique angles and result in foam deformation with both a shear and a compressive component. A test method to apply a combination of shear and compressive displacements to a foam sample has been developed. Furthermore, it is possible to analyze the shear and compressive components of deformation separately so that the coupling between shear and compressive behavior in cellular materials can be observed.

There has been other work in shear-compression testing devices for foam. However, these devices are all limited, not allowing for constant rates of shear and compression deformation, not allowing for the independent analysis of shear and compressive behavior under complex loading, or limiting the resultant angle of deformation [3-6]. The current work attempts to solve all of these problems for a more robust and useful shear-compression test.

While the application of this test is intended by the authors to be used for evaluating bicycle helmet foam, it could also be applied to any foam material that is expected to be loaded under both shear and compression. A possible example of this would be foam used for structural composite sandwich panels.

## 2 Experimental methodology

### 2.1 Development and validation of new test method

The test apparatus for this study was developed as an insert into an existing biaxial tensile/compression testing machine. This insert device allows for the testing of foams by the application of compression displacements along one machine axis and the application of shear displacements along the orthogonal axis (fig. 1). Each axis has an independent displacement actuator and an independent load cell. The displacement rate of each axis can be varied continuously from 0 (fixed) to 20 mm/min. This means that, theoretically, any resultant angle of deformation is possible from simple shear to pure compression (fig. 2).

The design of the apparatus is such that two blocks of foam are glued to 3 steel sample frames (fig. 1). The purpose of this symmetry is to avoid bending moments. The analysis, however, is conducted on only one foam block. Therefore, for calculations of shear and compressive stress, care must be taken to use the correct values. For calculating shear stress, *half* of the load output of the shear axis is used (since the foam blocks are loaded in parallel in shear) together with the dimensions of a single foam block. For compressive stress, the *entire* load output is used (since the foam blocks are loaded in series, and the sample setup is symmetric), together with the dimensions of a single foam block.

In order to validate the results of this machine, samples of construction foam material were tested in compression according to ASTM 1691, and in shear according to ISO 1922. The behavior of the foam was then compared to the data obtained by the experimental shear-compression testing device, when testing materials in compression (shear axis displacement set to 0 mm/min) and simple shear (compression axis displacement set to 0 mm/min). The data showed good correlation (figs. 3 and 4)

between the results obtained from the different test methods, and it was concluded that the new device provides reliable data in both shear and compression.

### 2.2 Materials and Methods

In this initial study, the behaviors of different foams are studied under shear-compression loading. State-of-the-art bicycle helmet grade expanded polystyrene (EPS) foam serves as the standard material in this study (fig. 5). This foam material has a density ($\rho_f$) of 75 kg/m$^3$. It is compared under shear-compression loading to a highly anisotropic polyethersulphone (PES) foam, selected to absorb comparable energy to the helmet grade EPS in drop impact tests. The PES foam is characterized by a shape anisotropy ratio, R, of approximately 10 (figs. 6 and 7), in contrast to the isotropic EPS. It is therefore expected to exhibit significantly lower shear resistance than the standard EPS material when tested under shear loading. The PES foam has a density ($\rho_f$) of 85 kg/m$^3$.

These different materials are tested over various loading angles from 0º (simple shear) to 90º (pure compression). Oblique angles tested include 15º, 30º, 45º, and 60º (fig. 2). The output of these tests is two simultaneous curves: a compressive stress-strain curve and a shear stress-strain curve. Because the strain rates in the two directions will be different (except in the case of 45º), the curves are first analyzed over the time domain (stress vs. time) in order to pinpoint the time in which one of the curves reaches a critical point (i.e. the end of the elastic region, a maximum design load, etc). The corresponding point in time on the other stress-time curve is determined (figs. 8 and 10), and then both curves are the analyzed up until the designated corresponding point in the strain domain (figs. 9 and 11).

### 3 Results

For application in bicycle helmets, the foam property that is of most interest is the energy absorption capacity of the foam up to the point that the stress exceeds a biomechanical limit. Stress is related to transmitted force, which is related to the acceleration or deceleration of the head during an impact. According to safety standards for bicycle helmet manufacture, which limit the maximum impact deceleration to 250 g's, this critical stress level is approximated as 1.12 MPa [7].

To understand how varying the angle of deformation affects the energy absorption properties of this foam, the following analysis was carried out. First, for each foam and each deformation angle, the time at which the compression curve exceeds a critical level was determined – point (1) in figures 8 and 10. The corresponding point in time in the shear curve was then found – point (2) in figures 8 and 10. The compressive and shear stress curves were then plotted in the strain domain (figs. 9 and 11), and the areas under the curve up until point (1) and (2) were determined. These are shown in figures 9 and 11 as the shaded areas (A) and (B). This was done for each material, and for each angle. Figures 12 and 13 show the stress-strain curves for an angle of 45º. It can be seen here that the compressive plateau is lower, compared to the curves of 60º, and also that the shear resistance is much higher. To understand how this affects the energy absorption of the foam, the absorbed energy as a function of angle of displacement can be analyzed. Figure 14 shows the energy that is absorbed due to the compression of the material (i.e. region (A) in figures 9 and 11) for all materials (not all curves are pictured). It is seen here that the compressive energy increases strongly from 60º to 45º (increasing shear) for the EPS material. This can be explained because the compressive plateau is decreasing with decreasing angle. Since the critical stress value at 60º lies within this plateau region, and moves further to the right with decreasing plateau strengths, more energy can be absorbed before reaching the critical stress. From 45º to 30º, the plateau stress decreases further, however, and a slight decrease in total absorbed energy is observed. For the PES material, the critical value is already at the end of the plateau region, so with decreasing plateau stress levels, the amount of energy that is absorbed decreases slightly over all 3 angles presented. In shear (fig. 15) it is clear that the EPS material, with a higher shear resistance, absorbs more energy than the PES material. Figure 16 shows the total energy that is absorbed (by adding the energies absorbed in compression and shear). We see that the helmet grade EPS absorbs more energy until a critical compressive stress than the PES material.

However, energy until a critical compressive stress only tells one side of the story. Figure 17 shows the shear stress when the compressive stress exceeds a critical value. This is also of interest, because it indicates the relative forces (tangential force at critical normal force) that would be transferred to

the head in an oblique impact situation. We can see here that, while EPS absorbs more total energy than PES up until a critical compressive value, it does so at a higher shear stress, which may lead to an increase in brain injuries that are caused by tangential forces or rotational accelerations.

Results of 0º and 90º tests have been omitted here in the interest of brevity, since these are simply standard shear and compression tests. 15º tests result have also been omitted, because there were significant problems with interface failure in these high shear tests. The glued interface failed before any critical stresses were reached, leading to a situation in which they could not be analyzed in the same method as the 60º, 45º, and 30º experiments.

## 4 Conclusions

The newly designed shear-compression testing apparatus that was used to carry out these experiments has been formally validated in both shear and compression by comparing results from this device to results using standard test methods on previously calibrated equipment.

The experimental analysis that was carried out for this study shows that the two types of materials exhibit different trends under changing angles of deformation.

For bicycle helmet cushioning foam, the critical point that was used as an upper bound in this analysis was either 1) a compressive stress of 1.12 MPa (which is based on calculations relating to the biomechanical limit in impact deceleration as stipulated by safety standards) or, 2) the point in which the compressive curve enters the densification region, where the stresses increase quickly and the behavior of bicycle helmets becomes unreliable. Helmets should be designed to absorb enough energy without exceeding 1.12 MPa or entering the densification region.

The differences in the compressive energy trends between the two materials can be attributed to the place in the curve where the material exceeds a critical value. The differences in the shear trends can be associated to the different shear stiffnesses of the materials, with EPS having an overall higher shear stiffness.

The critical value that was used as the upper bound for this analysis was in the compressive regime, but could have just as easily been defined as a critical value on the shear curve. If there are design limits in *both* the compressive and shear behaviors, it would be possible to make an analysis based on which curve exceeds a critical value first. Once more is known about the biomechanical limits of rotation (related to tangential forces and shear stresses) such that there can be a defined critical value in shear stress, this kind of "dual" analysis will need to be carried out for these materials for bicycle helmets.

This same analysis could be carried out for composite sandwich materials by using critical design loads for those applications, or to study mixed mode behavior and develop appropriate failure criteria for sandwich core materials.

## 5 Acknowledgements

This work was funded by the Flemish regional government through the *Fonds Wetenschappelijk Onderzoek (FWO) – Vlaanderen* (the Fund for Scientific Research – Flanders, Belgium).

## 6 Figures

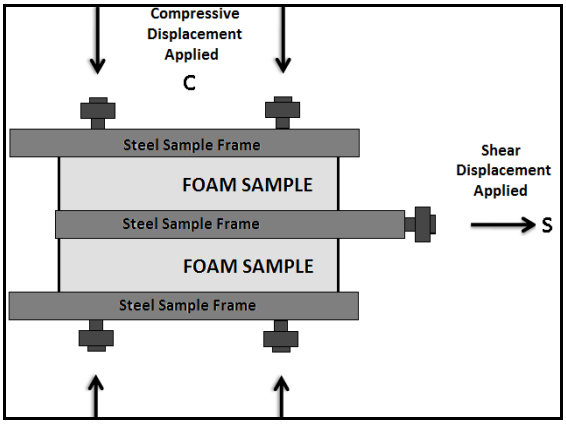


**Fig.1.** Graphical representation of the sample frame for shear-compression testing.

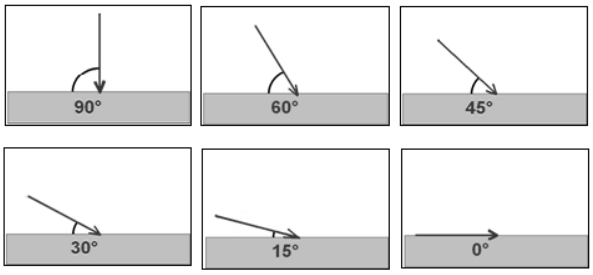


**Fig.2.** Diagram showing the resultant angle of deformation.

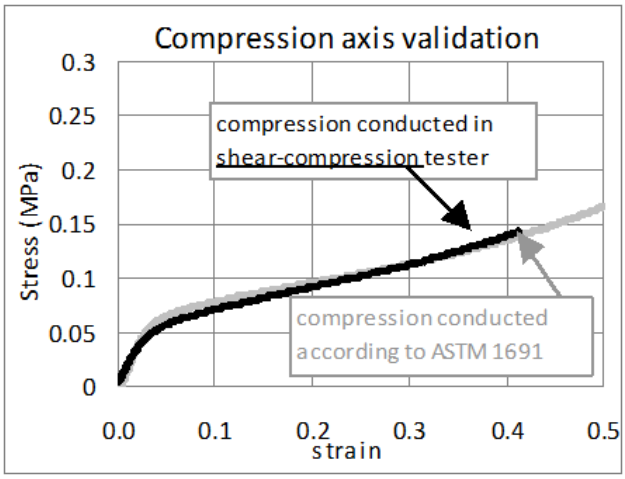


**Fig.3.** Compression test results for the validation of the new test setup. The close correlation of the data obtained in the compressive axis of the shear-compression tester (black) and the data obtained in a calibrated Instron tester according to ASTM 1691(grey), is within experimental sample scatter, and thus the acquired data is considered to be accurate in the compressive axis.

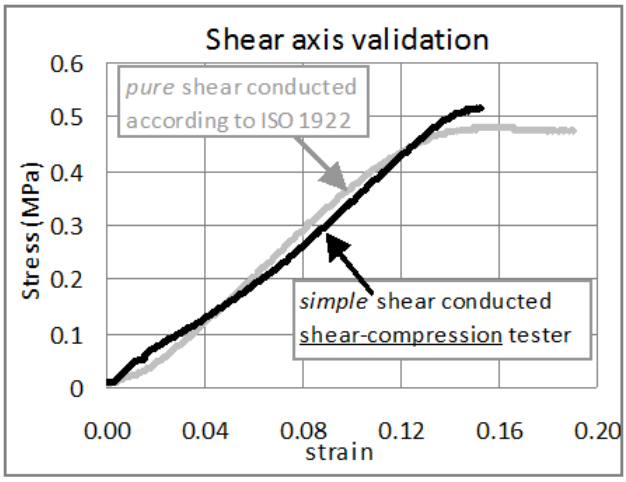


**Fig.4.** Shear test results for the validation of the new test setup. The close correlation of the data obtained from the shear axis of the shear-compression tester (black) and the data obtained in a calibrated Instron tester according to ISO 1922 (grey), is within experimental sample scatter, and thus the acquired data is considered to be accurate in the shear axis.

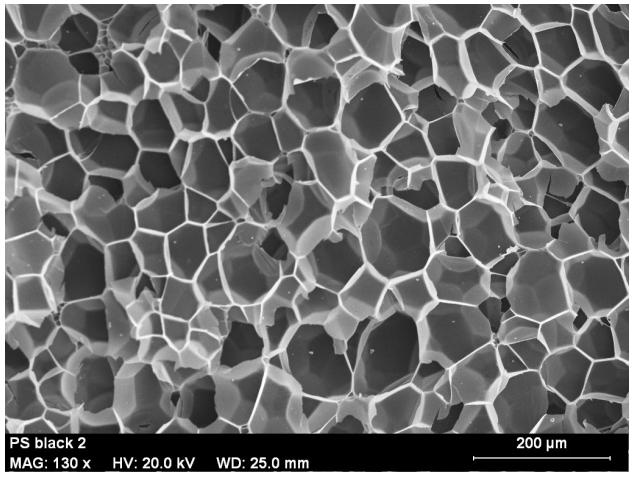


**Fig.5.** PES micrograph of isotropic EPS foam. The backs of the cells are visible here, unlike in figure 3.

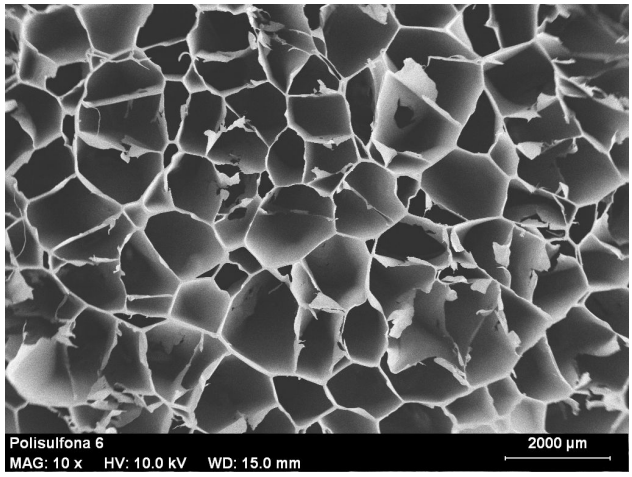


**Fig.6.** SEM micrograph of the anisotropic PES foam looking straight down through the length of the cells. *Note the difference in scale between the PES and EPS micrographs.*

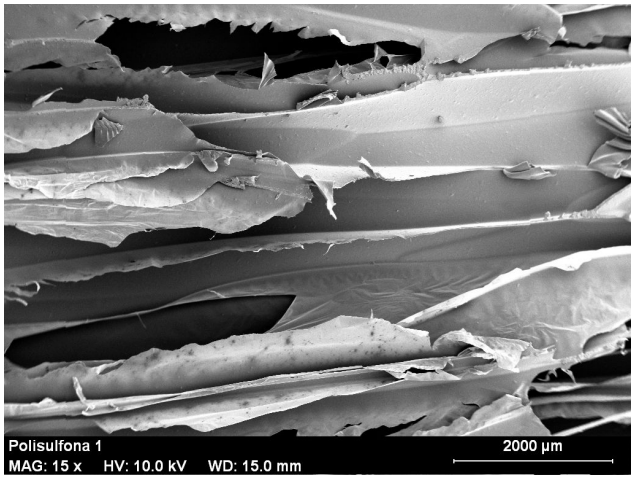


**Fig.7.** SEM micrograph of anisotropic PES foam looking along the length of the cells.

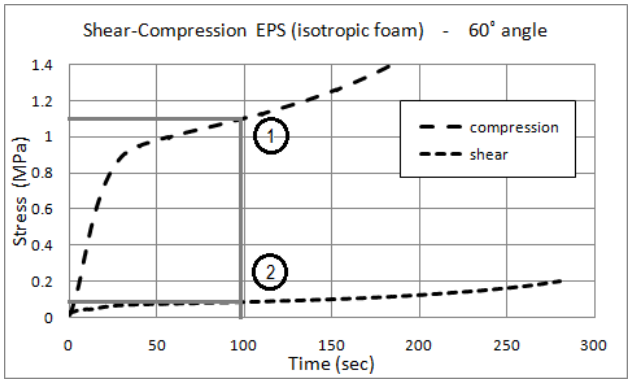


**Fig.8.** 60º shear-compression test of helmet grade EPS. The analysis is carried out until one of the curves reaches a critical value; in this case, the compressive curve reaches the biomechanical limit of 1.12 MPa at point (1). The corresponding point in time in the shear curve is determined, point (2).

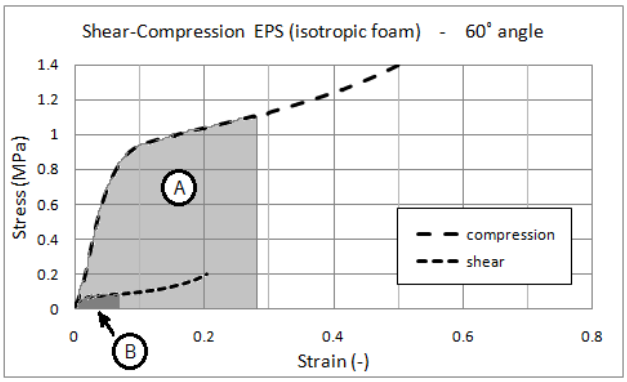


**Fig.9.** Points (1) and (2) are located on the stress-strain curve, and material properties can be determined at or until these points. For this analysis, the area under the curve, or the absorbed energy, was of interest. Areas (A) and (B), corresponding to the energy absorbed until points (1) and (2) were determined.

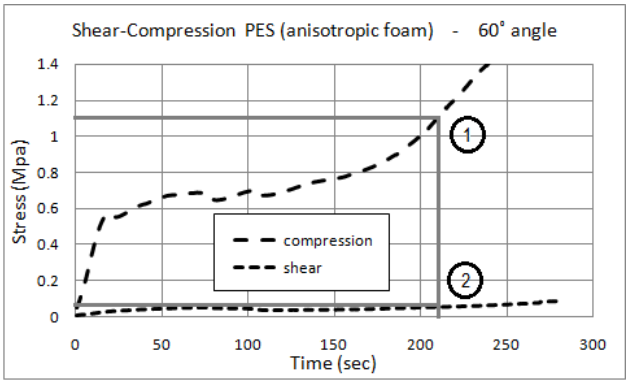


**Fig.10.** The same analysis as in figure 6 is carried out on the PES material. Points (1) and (2) are determined on the stress-time graphs.

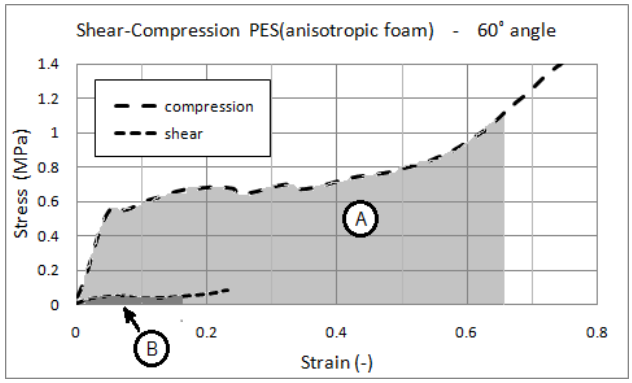


**Fig.11.** The areas under the curves, (A) and (B) are determined, indicating the energy that is absorbed in compression and shear up until points (1) and (2).

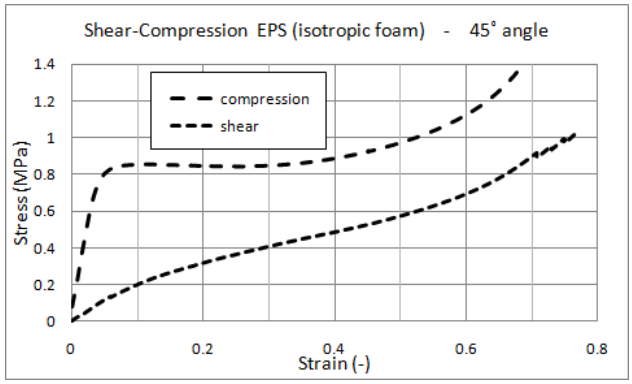


**Fig.12.** Compressive and Shear stress vs. strain curves for the EPS material at an applied displacement angle of 45º (equal rates of shear and compression displacement). The plateau stress of EPS at 45º is lower than that at 60º; however the shear resistance is much higher at 45º than at 60º.

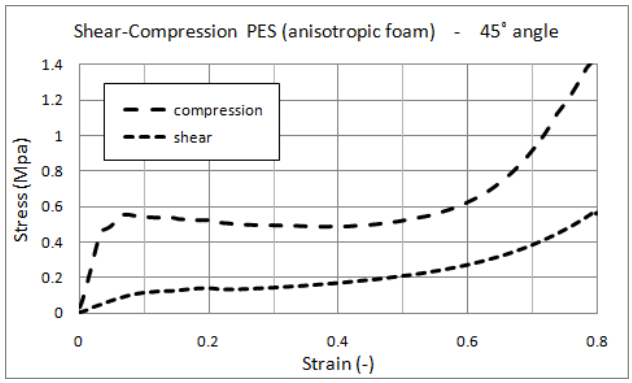


**Fig.13.** Compressive and Shear stress vs. strain curves for the PES material at an applied displacement angle of 45º. The plateau stress of PES at 45º is slightly lower than that it was at 60º. The shear resistance is higher at 45º than at 60º, however, at 45º the shear resistance of PES is still lower than the EPS material at 45º.

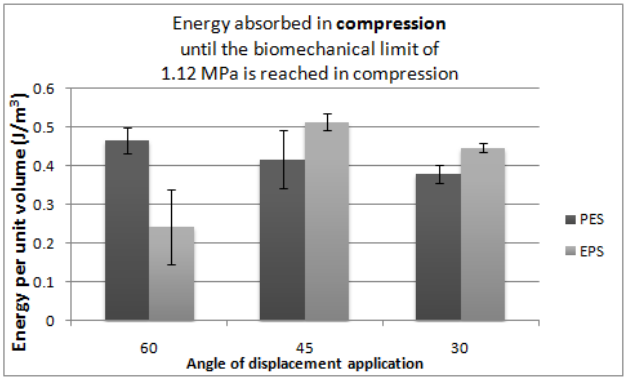


**Fig.14.** Energy absorbed in the foam material by compression for both materials, over 3 different angles of displacement.

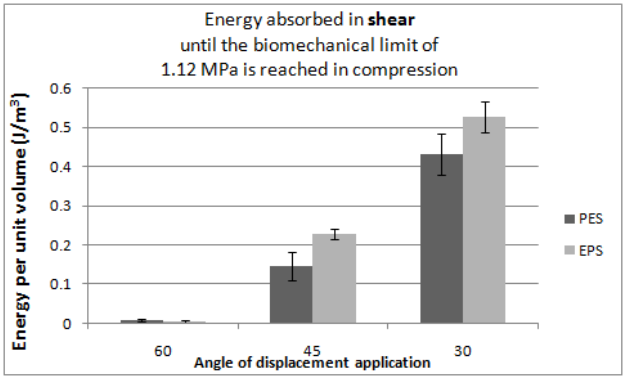


**Fig.15.** Energy absorbed in the foam material by shear for both materials, over 3 different angles of displacement.

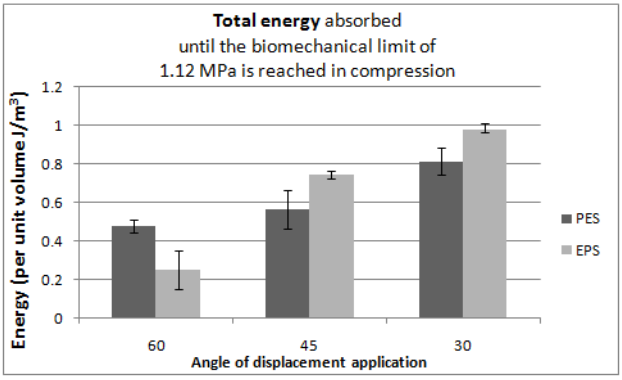


**Fig.16.** Total energy (from compression and shear) absorbed in the foam material for both materials, over 3 different angles of displacement.

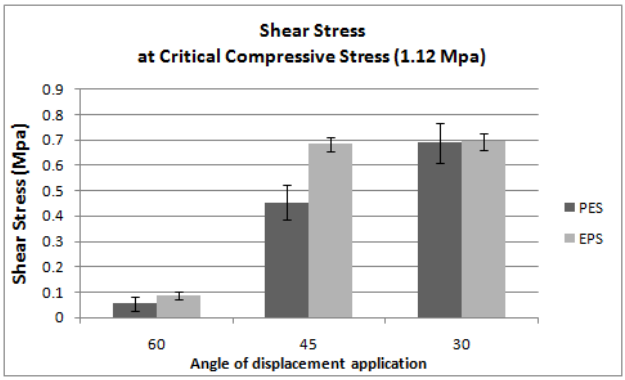


**Fig.17.** Shear stress when the compressive stress reaches the critical value of 1.12 MPa.

## References


[1] B. Depreitere, C. Van Lierde, S. Maene, C. Plets, J. Vander Sloten, R. Van Audekercke, G. Van der Perre, J. Goffin, J. "Bicycle-related head injury: a study of 86 cases". *Accident Analysis and Prevention.* Vol. 36, No. 4, pp 561-567, 2004.

[2] B. Depreitere, C. Van Lierde, J. Vander Sloten, R. Van Audekercke, G. Van der Perre, J. Goffin, J. "Mechanics of acute subdural haematomas resulting from bridging vein rupture". *Journal of Neurosurgery.* Vol. 104, pp.950-956, 2006.

[3] D. Benderly, S. Putter "Characterization of the shear/compression failure envelope of Rohacell foam". *Polymer Testing*. Vol. 23, No. 1, pp 51-57, 2004.

[4] M. Kintscher, L. Käger, A. Wetzel, D. Hartung, "Stiffness and failure behaviour of folded sandwich cores under combined transverse shear and compression". *Composites Part A: Applied Science and Manufacturing.* Vol. 38, No. 5, pp.1288-1295, 2007.

[5] M. Li, R. A.W. Mines, R. S. Birch, "The crush behaviour of Rohacell-51WF structural foam". *International Journal of Solids and Structures.* Vol. 37, No. 43, p.6321-6341, 2000.

[6] K. Chaimoon, M M. Attard. "Modeling of unreinforced masonry walls under shear and compression". *Engineering Structures*. Vol. 29, No. 9, p.2056-2068, 2007.

[7] K. Verjans. "Analyse van anisotrope schuimen onderworpen aan schuine impacts en quasi-statische afschuif-compressie belasting voor fietshelmtoepassingen". *Master's Thesis – Katholieke Universiteit Leuven, Belgium*. June 2010.